Available online at www.sciencedirect.com
SCIENCE DIRECT®
PERGAMON
Polyhedron 22 (2003) 2019–2025
POLYHEDRON
www.elsevier.com/locate/poly

Magnetic effective density functional studies on electronic states of $Cr_2(pyphos)_4$ and $Pt_2Cr_2(pyphos)_4(CH_3)_4$

Yasutaka Kitagawa [a,*], Shuhei Nakano [a], Takashi Kawakami [a], Kazushi Mashima [b], Kizashi Yamaguchi [a]

[a] *Chemistry Department, Graduate School of Science, Osaka University, Toyonaka, Osaka 560-0043, Japan*
[b] *Graduate School of Engineering Science, Osaka University, Toyonaka, Osaka 560-0043, Japan*

Received 6 October 2002; accepted 23 January 2003

Abstract

The effective exchange integral (J_{ab}) values between chromium ions in the aligned metal complexes; $Cr_2(pyphos)_4$ and $Pt_2Cr_2(pyphos)_4(CH_3)_4$ were investigated theoretically. Full model calculations presuming chromium(II) that were usually found in the $Cr_2(O_2CR)_4L_2$ complexes could not reproduce the small experimental J_{ab} values, suggesting another oxidation state of Cr. Several electronic states presuming Cr(III) were examined to explain the experimental J_{ab} values using naked model. The Cr(III) dimer model which had $\pi^4\delta^2$ triple bond showed small J_{ab} value that could explain experimental J_{ab} value of $Cr_2(pyphos)_4$. The calculated J_{ab} value presuming $\pi^4\delta^2$ triple bond of Cr(III) core also indicated appropriate J_{ab} values which could explain the very small experimental J_{ab} of $Pt_2Cr_2(pyphos)_4(CH_3)_4$. Natural orbital and instability analysis were performed to investigate such small J_{ab} value in $Pt_2Cr_2(pyphos)_4(CH_3)_4$. The conjugation of Pt–Cr–Cr–Pt core seemed to be effective in the decrease of J_{ab} between the Cr ions.

Keywords: One-dimensional (1D) metal chain complexes; Magnetic effective density functional, MEDF; Effective exchange integrals

1. Introduction

In recent years, many syntheses of one-dimensional metal chain complexes have been reported [1–6]. The metal–metal interactions in those complexes are characterized, metal species, bridging equatorial ligands and axial ligands [7]. It is supposed that each complex may have unique property by controlling the metal and ligand species. So, they are interesting in terms both of fundamental studies of their peculiar characters and applications to functional materials [8]. Many experimental studies have been carried out to know about their structures, magnetic and electronic properties [7,9]. Several theoretical studies also carried out to discuss their structural problems [7,10]. Details about their electronic structure, however, have not still been elucidated. We have studied about magnetic interactions between metal ions in those complexes by the theoretical calculation of the effective exchange integrals (J_{ab}) [11–14]. The magnetic properties in those complexes reflect the interaction between spins on metal ions. So, understanding of the magnetic interactions by the J_{ab} is very effective way to study the electronic states of these polynuclear complexes. It had been, however, difficult task to estimate J_{ab} accurately in those complexes, because they were too large to compute by post Hartree–Fock (HF) methods with an appropriate electron correlation. Furthermore, there was another problem that conventional density functional theory (DFT) methods such as B3LYP and BLYP overestimated J_{ab} values [12,15]. To overcome these problems we improved the hybrid DFT schemes, namely magnetic effective density functional (MEDF) method [15,16].

In this study, we focused on the aligned metal systems; $Cr_2(pyphos)_4$ (**2a**) where (pyphos = 6-(diphenylphosphino)-2-pyridonate) and $Pt_2Cr_2(pyphos)_4(CH_3)_4$ (**3a**) synthesized by Mashima et al. [1,2] as

* Corresponding author. Tel.: +81-6-6850-5405; fax: +81-6-6850-5550.
E-mail address: kitagawa@chem.sci.osaka-u.ac.jp (Y. Kitagawa).

0277-5387/03/$ - see front matter © 2003 Elsevier Science Ltd. All rights reserved.
doi:10.1016/S0277-5387(03)00215-8

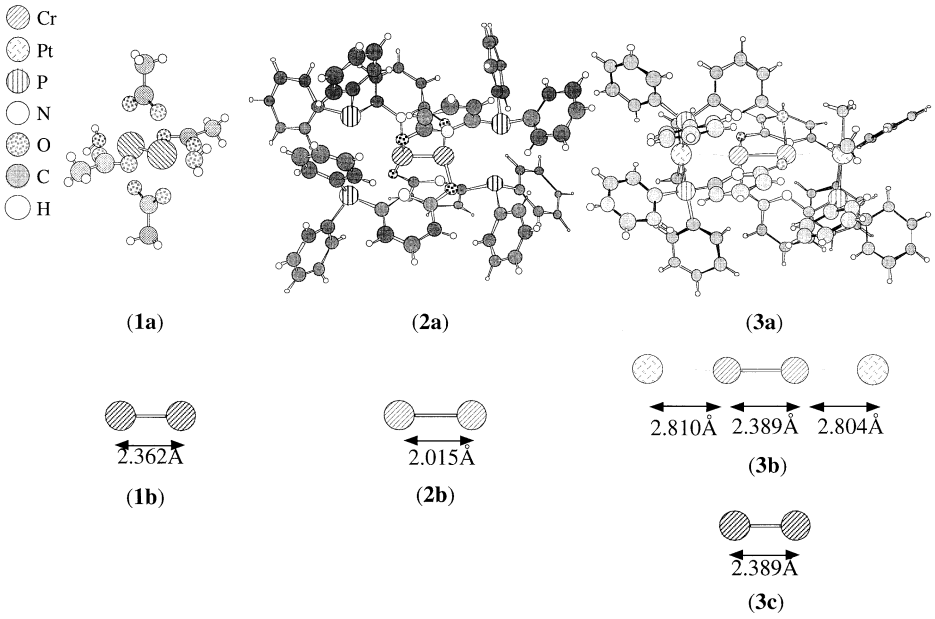

Fig. 1. Model figures of full model of $Cr_2(O_2CCH_3)_4(H_2O)_2$ (**1a**) and its naked Cr dimer model (**1b**) and full model of $Cr_2(pyphos)_4$ (**2a**), its Cr–Cr naked core model (**2b**). And model figures of full model of $Cr_2(pyphos)_4(CH_3)_4$ (**3a**), its naked Pt–Cr–Cr–Pt core model (**3b**) and its naked Cr–Cr model (**3c**).

illustrated in Fig. 1. $Pt_2Cr_2(pyphos)_4(CH_3)_4$ (**3a**) is interesting because different metal ions i.e. platinum ions coordinate to Cr–Cr core on its axis, where electron donors such as water are usually located [7]. Spin sources in those complexes were Cr ions and Cr–Cr distances of **2a** and **3a** were 2.015 and 2.389 Å, respectively. It has been supposed that the chromium ions in these complexes are Cr(II) and they have quadruple Cr–Cr bonds [1,2]. The details about electronic states of complex **2a** and **3a** have not been elucidated well. The experimental measurement revealed their small J_{ab} values in comparison with usual $Cr_2(O_2CR)_4L_2$ complexes [1,2]. J_{ab} values of **2a** observed by SQUID and NMR were -340 and -520 cm^{-1}, respectively [1,2]. While observed J_{ab} value of **3a** was -29 cm^{-1} [1,2]. At first, we verified the MEDF method using fundamental complex $Cr_2(O_2CCH_3)_4(H_2O)_2$ (**1a**) and its naked Cr(II) dimer model (**1b**). Next, we applied the MEDF method to **2a**, **3a** and their naked core models to calculated J_{ab} values. We discussed the electronic states of these complexes with calculated J_{ab} values between Cr ions.

2. Theoretical background

2.1. Magnetic effective density functional method

The MEDF method takes an appropriate dynamical correlation effect into account by DFT terms, based on the approximation that a non-dynamical correlation is expressed by using unrestricted calculation [15,16]. In the MEDF method, the exchange-correlation potential, which involved both HF and DFT terms was generalized as follows [16];

$$E_{XC} = c_1 E_X^{HF} + (1 - c_1) E_X^{DFT} + E_C^{DFT} \quad (1)$$

$$E_{XC} = c_1 E_X^{HF} + (1 - c_1)(E_X^{LSDA} + \Delta E_X^{GGA}) + E_C^{LSDA} + \Delta E_C^{GGA} \quad (2)$$

where Slater's exchange functional [19], Becke's exchange functional [20], VWN correlation function [21] and LYP correlation functional [22] were used as E_x^{LSDA}, ΔE_X^{GGA}, E_C^{LSDA} and ΔE_C^{GGA}, respectively. If two spins have little interaction such as fully dissosiated H_2 molecule, the spin interaction energy is estimated by unrestricted HF (UHF) because dynamical correlation effect between the spins is negligible. While dynamical correlation effect must be corrected if there is interaction between spins. MEDF method corrects this dynamical correlation energy by DFT terms. The mixing coefficient was estimated by the instabilities in chemical bonds that express the magnitude of spin interactions [16].

2.2. Computational details

In those calculations, we used Heisenberg model (in Eq. (3)) and size-consistent spin projection (in Eq. (4)) to estimate J_{ab} [15,17,18].

$$H = -2 \sum J_{ab} \mathbf{S_a} \cdot \mathbf{S_b} \quad (3)$$

$$J(AP - Z) = \frac{^{LS}E(Z) - {}^{HS}E(Z)}{^{HS}\langle S^2\rangle(Z) - {}^{LS}\langle S^2\rangle(Z)} \quad (4)$$

where ^{Y}E and $^{Y}\langle S^2\rangle$ denoted the total energy and total

angular momentum of the spin state Y. Those spin projected J_{ab} values calculated by the method Z called AP–Z such as APUHF. All atomic coordinations except for hydrogen atoms were taken from date of X-ray crystal structure analyses. Hydrogen atoms were added based on the general chemical bonds. Those calculations were performed by the use of Tatewaki–Huzinaga MIDI (533(21)/53(21)/(41)) [23] for Cr, Pt and 4-31G basis sets for other atoms. All calculations were carried out by using GAUSSIAN-98 [24].

3. Results and discussion

3.1. Verification of MEDF and approximated spin projection

At first, a effectiveness of the MEDF for J_{ab} values were examined here using $Cr_2(O_2CCH_3)_4(H_2O)_2$ (**1a**) and its naked dimer model (**1b**) as illustrated in Fig. 1.

Cr(II)–Cr(II) distance in this complex is 2.362 Å and experimental J_{ab} values is $-490\ cm^{-1}$ [7]. The electronic state of this complex is described using MO picture as follows; $(\sigma)^2(\pi)^4(\delta)^2$ for low spin state ($S=0$) and $(\sigma)^1(\pi)^2(\delta)^1(\delta^*)^1(\pi^*)^2(\sigma^*)^1$ for high spin state ($S=4$). Theoretical calculations also reproduced the electronic state. Calculated results were compared with experimental J_{ab} value for **1a** and J_{ab} value by UCCSD(T) that took single, double and triple excitations into account for **1b**. Table 1 summarized them.

MEDF method could reproduce not only J_{ab} value of UCCSD(T) method for naked dimer model **1b** but also the experimental J_{ab} value for **1a**. UHF underestimated J_{ab} value because electron correlation effects were not considered enough especially for a singlet state. On the other hand, conventional UBLYP and UB3LYP overestimated J_{ab} value because they were optimized for stable closed shell systems [15,16]. Andersson et al. obtained S–T gap 983 cm^{-1} ($J_{ab}=-491.5\ cm^{-1}$) that perfectly agreed with the experimental values using complete active space self consistent field second-order perturbation theory eight-space, eight-electron (CASPT2{8,8}) calculations [10]. However, complete active space configuration interaction (CASCI{8,8}) calculation underestimated J_{ab} value [12]. Here, CAS space was valence orbital that mainly consisted of d-orbital of Cr(II) ions i.e. $(\sigma)^2(\pi)^4(\delta)^2$ for low spin state ($S=0$) and $(\sigma)^1(\pi)^2(\delta)^1(\delta^*)^1(\pi^*)^2(\sigma^*)^1$ for high spin state ($S=4$) [13]. These results indicated that dynamical correlation correction for inner electrons was necessary. Different from the CASPT2 which include dynamical correlation by MP2 and non-dynamical correlation by CAS, the MEDF is a method that an appropriate dynamical correlation effect into account by DFT terms, based on the approximation of non-dynamical correlation using unrestricted calculation, as explained in previous section [16]. Therefore MEDF can calculate J_{ab} values with less computational costs. For large systems such as polynuclear systems, the CASPT2 calculation is difficult to perform because of computational costs. So, the MEDF approach approximately substitutes for CASPT2 level in those complexes. From these results, we could verify that J_{ab} values calculated by MEDF reproduced J_{ab} values between Cr(II) ions in a di-Cr(II) tetraacetate complex (**1a**) and it is naked metal dimer model (**1b**).

The CASCI{8,8} calculation must contain the magnetic interaction of valence electrons between Cr(II) ions, in other words, 'd–d direct interaction' because active space were consisted of Cr(II)–Cr(II) quadruple bonding and their anti-bonding orbitals. So, the meaning of the difference between calculated CASPT2 and DNO-CASCI{8,8}, i.e.

$$\Delta J = J(\mathrm{CASPT2}\{8,8\})\text{-}J(\mathrm{CASCI}\{8,8\}) \quad (5)$$

mainly comes from the through-ligand interaction. If we approximate

$$J(\mathrm{CASPT2}\{8,8\}) \equiv J(\mathrm{MEDF}) \quad (6)$$

then

$$\Delta J' = J(\mathrm{MEDF}) - J(\mathrm{CASCI}\{8,8\}) \quad (7)$$

is approximately expressing the through-ligand interaction. In this way, we could estimate the through-ligand interaction as $-190\ cm^{-1}$. The estimated through-ligand interaction was negative and bridging ligand contributed to anti-ferromagnetic interaction. J(CASCI{8,8}) was close to naked J_{ab} by MEDF. This suggested that the effect of ligand for the d–d direct interaction was relatively small.

Table 1
Effective exchange integrals (J_{ab}) values [a] of $Cr_2(O_2CCH_3)_4(H_2O)_2$ (**1a**) and its naked dimer model (**1b**)

Method	1a	1b
APUHF	−281	−151
MEDF [b]	−520	−299
APUB3LYP	−733	−402
APUBLYP	−1042	– [c]
APUCCSD(T)		−210
Experiment	−490	

[a] In cm^{-1}.
[b] $c_1=0.5$ in Eq. (2).
[c] Appropriate electronic state could not obtained by UBLYP.

3.2. J_{ab} calculations presuming Cr(II)

Next, we calculated J_{ab} values of $Cr_2(pyphos)_4$ (**2a**) presuming Cr(II) and calculated electronic states are described using MO picture as follows; $(\sigma)^2(\pi)^4(\delta)^2$ for low spin state ($S=0$) and $(\sigma)^1(\pi)^2(\delta)^1(\delta^*)^1(\pi^*)^2(\sigma^*)^1$ for

high spin state ($S = 4$), which were similar to **1a**. SQUID and NMR measurements indicated different J_{ab} values that were -340 and -540 cm^{-1}, respectively [1,2]. The both values were smaller than usual J_{ab} value between Cr(II) ion at a distance of 2.015 Å [7,15,16]. Here, we calculated J_{ab} values of the full model (**2a**) and naked dimer core model (**2b**) as illustrated in Fig. 1. The calculated results were summarized in Table 2.

All calculated J_{ab} values indicated anti-ferromagnetic interactions between Cr(II). The calculated J_{ab} values of naked dimer model **2b**, however, were larger than experimental values. The J_{ab} value calculated by the MEDF method of $c_i = 0.5$ in Eq. (2) that was optimized for the Cr(II) dimer [12] close to J_{ab} by the UCCSD(T). In previous section, we pointed out that bridging ligand contributed to anti-ferromagnetic interaction in **1a**. So, it was inconsistent with **1a** and inexplicable that J_{ab} of naked dimer model was larger than experimental value. The J_{ab} value of full model (**2a**) was calculated by using UHF and MEDF. We found that calculated J_{ab} values were about twice as large as experimental J_{ab} values. The J_{ab} between Cr(II) ions estimated by the S–T gap plot by Cotton et al. was about 1000 cm^{-1} at a distance of 2.0 Å [9]. The J_{ab} value by MEDF (-1202 cm^{-1}) was consistent with it. So, it was conceived that MEDF reproduced J_{ab} between Cr(II) ions in full model, well. To obtain a molecular orbital (MO)-like picture, the natural orbital (NOs) of the MEDF for singlet state were depicted in Fig. 2, and we confirmed that calculated electronic state, which consisted of the $(\sigma)^2(\pi)^4(\delta)^2$ orbitals, was not incorrect.

From these results, we could not explain experimental J_{ab} values of **2a** presuming that Cr ions in **2a** were $+2$ cation, leading a possibility that Cr ions were not Cr(II).

The difference between J_{ab} of full model (**2a**) and naked core model (**2b**) estimated by MEDF was about -330 cm^{-1}. This anti-ferromagnetic coupling through-ligand was consistent with **1a**. J_{ab} through-ligand seemed to be considerably large. At least, J_{ab} by Cr–Cr direct interaction in **2a** should be smaller than experimental J_{ab} value, -540 cm^{-1}.

Next, we examine J_{ab} of $Pt_2Cr_2(pyphos)_4(CH_3)_4$ (**3a**). It was reported that this complex showed extremely small J_{ab} (-29 cm^{-1})[1,2] as compared with usual J_{ab} value between Cr(II) ion at a distance of 2.389 Å [7,15,16]. Here, we also presumed that Cr and Pt ions were $+2$. The calculated results were summarized in Table 3.

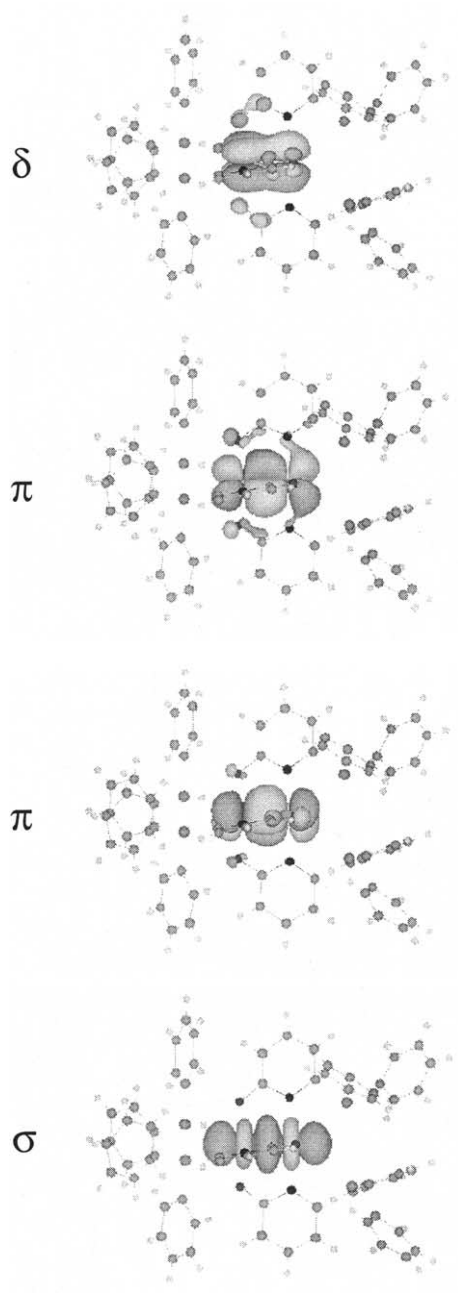

Fig. 2. NOs for σ, π and δ orbitals of $Cr_2(pyphos)_4$ (**2a**) presuming Cr(II).

Table 2
Effective exchange integrals (J_{ab}) [a] between Cr(II) ions in $Cr_2(pyphos)_4$ (**2a**) and its naked core model (**2b**)

Method	2a	2b
APUHF	−739	−532
MEDF [b]	−1202	−870
APUMP2		−607
APUMP4(SDTQ)*		−644
APUCCSD(T)		−831
UNO-CASCI[8,8]		−656
Experiment	−340 [c], −540 [d]	

[a] In cm^{-1}.
[b] $c_1 = 0.5$ in Eq. (2).
[c] SQUID value in Refs. [1,2].
[d] NMR value in Ref. [2].

Table 3
Effective exchange integrals (J_{ab}) [a] between Cr(II) ions in $Pt_2Cr_2(pyphos)_4(CH_3)_2$ (**3a**), its naked Pt–Cr–Cr–Pt core model (**3b**) and its naked Cr–Cr core model (**3c**)

Method	3a	3b	3c
APUHF	−185	−103	−136
MEDF [b]	−407	−178	−275
APUMP2		−126	−155
APUMP4(SDTQ)		−135	−164
APUCCSD(T)			−189
Experiment	−29 [c], −10 [d]		

[a] In cm^{-1}.
[b] $c_1 = 0.5$ in Eq. (2).
[c] SQUID in Refs. [1,2].
[d] NMR in Ref. [1].

In every model of Cr–Cr naked core (**3c**), Pt–Cr–Cr–Pt naked core (**3b**) and complex (**3a**), the calculated J_{ab} values were larger than the experimental value. The J_{ab} between Cr(II) ions estimated by the S–T gap plot by Cotton et al. was about -450 cm^{-1} at a distance of 2.4 Å [9]. Calculated J_{ab} by MEDF (-407 cm^{-1}) was consistent with it. In these models, we could not reproduce and explain the experimental J_{ab} values of **3a** presuming that Cr and Pt were +2 cation, again.

The existence of Pt(II) ions decreased J_{ab} value between Cr(II) ions in comparison with J_{ab} of **3b** and **3c**. This meant that Pt(II) ions made Cr(II)–Cr(II) bond unstable and the interaction between spins on Cr(II) ions decreased.

3.3. J_{ab} calculation presuming of Cr(III)

Here, we examined the possibility of Cr(III) in $Cr_2(pyphos)_4$ (**2a**) and $Pt_2Cr_2(pyphos)_4(CH_3)_4$ (**3a**) to explain the experimental J_{ab} values, using their naked models (**2b**), (**3b**) and (**3c**) as illustrated in Fig. 1. As mentioned in previous section, the MOs of valence electrons, which causes d–d direct interaction are similar to ones of full model. So, we these J_{ab} values should be smaller than experimental values because naked dimer model does not have equatorial ligands that contributes to anti-ferromagnetic coupling between Cr ions. There were three candidates of the electron configuration for Cr(III)–Cr(III) triple bonds; $\sigma^2\pi^2\delta^2$, $\sigma^2\pi^4$, and $\pi^4\delta^2$. We calculated J_{ab} values for each electronic configuration.

At first, we calculated J_{ab} values of $Cr_2(pyphos)_4$ (**2a**) presuming Cr(III). The calculated J_{ab} values of $\sigma^2\pi^2\delta^2$, $\sigma^2\pi^4$, and $\pi^4\delta^2$ configurations were summarized in Table 4.

J_{ab} values were smaller than one's of naked Cr(II) dimer model in Table 2, except for $\sigma^2\pi^4$ state. Their order was $|J_{ab}(\sigma^2\pi^4)| > |J_{ab}(\sigma^2\pi^2\delta^2)| > |J_{ab}(\pi^4\delta^2)|$. This tendency reflected the stability of chemical bonds; $\sigma > \pi > \delta$ because the stable chemical bonds contributed to large negative J_{ab} values [15,16]. For example, the calculated $J_{ab}(\pi^4\delta^2)$ was small because the $\pi^4\delta^2$ state did not have σ bonding which gave large negative J_{ab} value. These naked models did not take through-ligand effects into account. We found through-ligand effects in (**2b**) was relatively large presuming Cr(II). So, possible candidate of electronic state of $Cr_2(pyphos)_4$ seemed to be $\pi^4\delta^2$ state of Cr(III) dimer core that had smallest J_{ab} value. However a possibility of $\sigma^2\pi^2\delta^2$ could not deny because it has smaller J_{ab} value than the experimental value. There was little possibility of the $\sigma^2\pi^4$ state of Cr(III) dimer core that had larger J_{ab} value than the experimental value.

Next, the electronic state of $Pt_2Cr_2(pyphos)_4(CH_3)_4$ was also examined by using Cr–Cr naked core model (**3c**) and Pt–Cr–Cr–Pt naked core model (**3b**) assuming Pt(II) and Cr(III), respectively. These calculations, however, were very difficult to converge. So, we substituted point charges for ligand atoms. Only the atoms that had connections to metal ions (P, N,O atoms of pyphos ligands and C atoms of CH_3 ligands) were used as point charges and they were based on the calculated results of $pyphos^-$ and CH_3^- by RHF. They were located on same arrangement with real complex (**3a**). Here, we calculated J_{ab} values of $\sigma^2\pi^2\delta^2$ and $\pi^4\delta^2$ configurations of Cr(III)–Cr(III) core because they were candidates for the electronic state for $Cr_2(pyphos)_4$. The results were summarized in Table 5.

In comparison with the data of $Cr_2(pyphos)_4$ in Table 4, calculated J_{ab} values were decreased drastically. Especially, J_{ab} value by APUHF was slightly positive in case of $\pi^4\delta^2$ state of **3b**. Because of the suggestion that Cr–Cr direct exchange interactions must be very small from the estimation of through-ligand J_{ab} presuming Cr(II), we concluded that the $\pi^4\delta^2$ configurations of Cr(III)–Cr(III) core was the possible candidate for $Pt_2Cr_2(pyphos)_4(CH_3)_4$.

Table 4
Effective exchange integrals (J_{ab}) [a] between Cr(II) ions of several electronic states in naked core model (**2b**)

Method	$\sigma^2\pi^4$	$\sigma^2\pi^2\delta^2$	$\pi^4\delta^2$
APUHF	−629	−423	−263
MEDF [b]	−1018	−679	−423
APUCCSD(T)	−527		−278
APUMP2	−678	−449	−347
APUMP4(STDQ)	−705	−465	−285
Experiment (**2a**)	−340 [c], −540 [d]		

[a] In cm^{-1}.
[b] $c_1 = 0.5$ in Eq. (2).
[c] SQUID in Ref. [1].
[d] NMR in Ref. [2].

Table 5
Effective exchange integrals (J_{ab}) [a] between Cr(III) ions of several electronic states in naked Pt–Cr–Cr–Pt core model (**3b**) and naked Cr–Cr core model (**3c**) of $\sigma^2\pi^2\delta^2$ and $\pi^4\delta^2$ states

Method	$\sigma^2\pi^2\delta^2$		$\pi^4\delta^2$	
	(**3b**)	(**3c**)	(**3b**)	(**3c**)
APUHF	−74	−77	10	−33
APUMP2	−83	−82	−17	−35
APUMP4(SDTQ)	−84	−84	−31	−36
Experiment	−29 [b]			

[a] In cm^{-1}.

To clarify such a peculiar J_{ab} of the $\pi^4\delta^2$ state, we analyzed its NOs and instabilities of orbitals as illustrated in Fig. 3.

Instabilities of each orbitals were estimated by using the information entropy. There are some attempts to apply the information theory to the studies of atomic and molecular systems. Ramílez et al. [25] indicated that the entropy of the system is calculated as follows;

$$I = -\sum_i n_i \ln n_i \tag{8}$$

Here n_i is occupation number of occupied NO. We improved it as follows [16];

$$I' = 1 - \frac{n_i \ln n_i}{2 \ln 2} \tag{9}$$

This normalized information entropy; I' indicates zero in the region strong bonding region while it indicates 1.0 in fully dissociated region. Here, we used this I' to estimate the instabilities of metal–metal bonds. Calculated I' of **3b** by UHF was summarized in Table 6.

Table 6
Occupation numbers and instability values [a,b] of magnetic orbitals of **2b**, where Cr(III)–Cr(III) core was $\pi^4\delta^2$ configuration calculated by UHF

Orbital	Occupation number	Instability value
HOMO	1.00544	99.6 (99.5)
HOMO-1	1.02070	98.5 (96.5)
MOHO-2	1.03189	97.7 (96.5)
MOHO-3	1.04975	96.3
HOMO-4	1.06322	95.3
MOHO-5	1.98730	1.55
HOMO-6	1.99096	1.10
MOHO-7	1.99920	0.0977
MOHO-8	1.99964	0.0440
HOMO-12	1.99998	0.00244
HOMO-13	1.99999	0.00122

[a] In (%).
[b] Instability values of **2c** were written in parentheses.

From the pictures of NOs as illustrated in Fig. 3, we found that HOMO was Cr–Cr δ bond. While HOMO-1 to HOMO-4 were conjugated orbitals of Cr–Cr π bonds and Pt(II)'s orbital. It was considered that interaction between Pt and Cr–Cr center was week because there were dδ-like component of Pt(II)'s orbital and overlap between Pt and Cr–Cr center was small. This dδ component of Pt(II) reflected the effects of point charges. Instability values of these HOMO to HOMO-5 orbitals in Table 6 were more than 95%. Especially, HOMO-1 and HOMO-2 that were originated in π orbitals of Cr–Cr bonding increased their instabilities in comparison with **2c** (see values in parentheses). This instability contributed to the decrease of J_{ab} of **3b**. HOMO-5 to HOMO-8 and HOMO-12, HOMO-13 orbitals were mainly derived from Pt(II)'s orbitals. HOMO-5 and HOMO-6 orbitals were σ-type orbitals that derived from Pt(II)'s orbitals and they were slightly

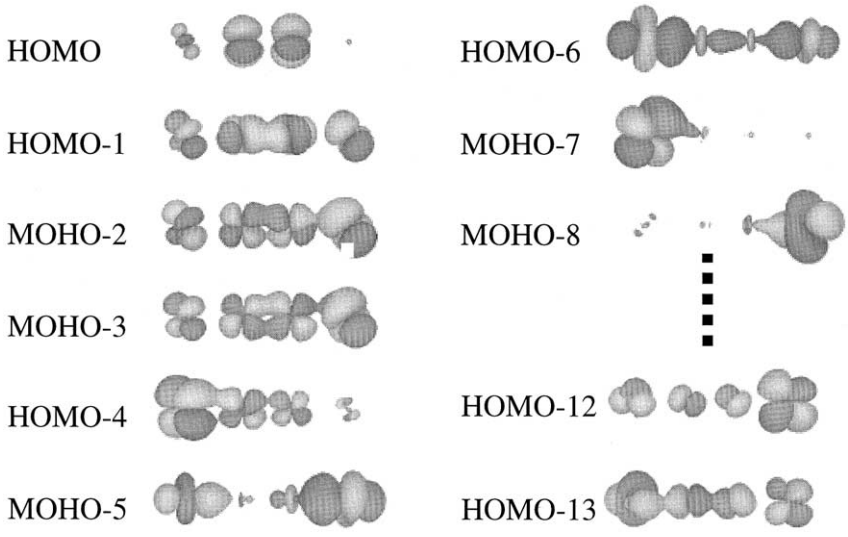

Fig. 3. NOs of naked Pt–Cr–Cr–Pt core model (**3b**) of $\pi^4\delta^2$ state.

unstable. The vacant σ orbital of Cr–Cr core contributed to this instability of Pt(II)'s σ-type orbital.

4. Concluding remarks

We studied the electronic states of $Cr_2(pyphos)_4$ (**2a**) and $Pt_2Cr_2(pyphos)_4(CH_3)_4$ (**3a**) by using J_{ab} values. The calculated values of **2a** and **3a** did not reproduce experimental J_{ab} presuming Cr(II). Therefore we considered a possibility of another oxidation states of Cr in those complexes to explain experimental J_{ab} values. We, next, carried out the J_{ab} calculations by using naked models, presuming Cr(III). $\pi^4\delta^2$ triple bonded state gave smallest J_{ab} than $\sigma^2\pi^2\delta^2$ and $\sigma^2\pi^4$ in the **2b** model. This $\pi^4\delta^2$ triple bonded state seemed to be possible candidate for the electronic states of **2a**. In the **3b** model, electronic state which involved $\pi^4\delta^2$ triple bonded Cr(III)–Cr(III) core gave slightly positive J_{ab} values by APUHF calculation. This was good agreement with experimental result, which showed very small J_{ab}. The electronic state which involved $\pi^4\delta^2$ triple bonded Cr(III)–Cr(III) core also seemed to be possible candidate for the electronic states of **3a**. It should be emphasized again that we presented the possibility of electronic state for $Cr_2(pyphos)_4$ and $Pt_2Cr_2(pyphos)_4(CH_3)_4$. $\pi^4\delta^2$ core of Cr(III) dimer in those complexes was just the candidates to explain such a small J_{ab} values. Full model calculations presuming Cr(III) are necessary for further investigation.

NO analysis and the instability analysis were performed to explain its peculiar J_{ab}. The π bonding orbitals of Cr(III)–Cr(III) core and the orbital of Pt(II) were conjugated. Instability values of the π type conjugated orbitals and the δ bonding orbital of Cr(III)–Cr(III) core were more than 95% and π orbitals of Cr(III)–Cr(III) core were unstabilized by the existence of Pt(II). The instability of these π conjugations seemed to contribute to the small J_{ab} values of **3c**. From these results, we found that Cr–Cr σ bond have great influence on J_{ab}. By withdrawing electrons from σ orbital of Cr(II)–Cr(II) quadruple bond, J_{ab} values in di-chromium complexes decreases significantly. In this study, we demonstrated that calculated J_{ab} clued us in about the unknown electronic states of complexes.

Acknowledgements

This work has been supported by a Grant-in-Aid for Scientific Research on Priority Areas (Nos. 14204061 and 13740396) from Ministry of Education, Culture, Sports, Science and Technology, Japan. One of the author Y.K has been assisted by the Research Fellowship of the Japan Society for the Promotion of Science for Young Scientists.

References

[1] K. Mashima, M. Tanaka, K. Tani, J. Am. Chem. Soc. 119 (1997) 4307.
[2] M. Tanaka, K. Mashima, M. Nishino, S. Takeda, W. Mori, K. Tani, K. Yamaguchi, A. Nakamura, Bull. Chem. Soc. Jpn. 74 (2001) 67.
[3] F.A. Cotton, L.M. Daniels, C.A. Murillo, X. Wang, Chem. Commun. (1998) 39.
[4] S.-Y. Lai, T.-W. Lin, Y.-H. Chen, C.-C. Wang, G.-H. Lee, M.-H. Yang, M.-K. Leung, S.-M. Peng, J. Am. Chem. Soc. 121 (1999) 250.
[5] M.E. Prater, L.E. Pence, R. Clérac, G.M. Finniss, C. Campana, P. Auban-Senzier, D. Jérome, E. Canadell, K.R. Dunber, J. Am. Chem. Soc. 121 (1999) 8005.
[6] C. Bellitto, G. Dessy, V. Fares, Inorg. Chem. 24 (1985) 2815.
[7] F.A. Cotton, R.A. Walton, Multiple Bonds between Metal Atoms (and references therein), Clarendon Press, Oxford, 1993.
[8] M.H. Chisholm, Acc. Chem. Res. 33 (2000) 53.
[9] F.A. Cotton, H. Chen, L.M. Daniels, X. Feng, J. Am. Chem. Soc. 114 (1992) 8980.
[10] K. Andersson, C.W. Bauschlicher, Jr., B.J. Persson, B.O. Roos, Chem. Phys. Lett. 257 (1996) 238.
[11] M. Nishino, S. Yamanaka, Y. Yoshioka, K. Yamaguchi, J. Phys. Chem. A 101 (1997) 705.
[12] Y. Kitagawa, T. Soda, T. Onishi, Y. Takano, M. Nishino, Y. Yoshioka, K. Yamaguchi, Mol. Cryst. Liq. Cryst. 343 (2000) 463.
[13] Y. Kitagawa, T. Kawakami, Y. Yoshioka, K. Yamaguchi, Polyhedron 20 (2001) 1189.
[14] Y. Kitagawa, M. Nishino, Y. Kawakami, Y. Yoshioka, K. Yamaguchi, Mol. Cryst. Liq. Cryst. 376 (2002) 347.
[15] Y. Kitagawa, T. Soda, Y. Shigeta, S. Yamanaka, Y. Yoshioka, K. Yamaguchi, Int. J. Quant. Chem. 84 (2001) 592.
[16] Y. Kitagawa, T. Kawakami, K. Yamaguchi, Mol. Phys. 100 (2002) 1829.
[17] K. Yamaguchi, Y. Takahara, T. Fueno, in: V.H. Smith, H.F. Schaefer, III, K. Morokuma (Eds.), Applied Quantum Chemistry, D. Reidel Pub. Co, Boston, 1986, p. 155.
[18] K. Yamaguchi, in: R. Carbo, M. Klobukowski (Eds.), Self-Consistent Field Theory and Applications, Elsevier, Amsterdam, 1990, p. 727.
[19] J.C. Slater, Quantum Theory of Molecular and Solids. The Self-Consistent Field for Molecular and Solids, vol. 4, McGraw-Hill, New York, 1974.
[20] A.D. Becke, Phys. Rev. A 38 (1988) 3098.
[21] S.H. Vosko, L. Wilk, M. Nusair, Can. J. Phys. 58 (1980) 1200.
[22] C. Lee, W. Yang, R.G. Parr, Phys. Rev. B 37 (1988) 785.
[23] H. Tatewaki, S. Huzinaga, J. Chem. Phys. 71 (1979) 4339.
[24] GAUSSIAN-98, M.J. Frisch, G.W. Trucks, H.B. Schlegel, G.E. Scuseria, M.A. Robb, J.R. Cheeseman, V.G. Zakrzewski, J.A. Montgomery, Jr., R.E. Stratmann, J.C. Burant, S. Dapprich, J.M. Millam, A.D. Daniels, K.N. Kudin, M.C. Strain, O. Farkas, J. Tomasi, V. Barone, M. Cossi, R. Cammi, B. Mennucci, C. Pomelli, C. Adamo, S. Clifford, J. Ochterski, G.A. Petersson, P.Y. Ayala, Q. Cui, K. Morokuma, N. Rega, P. Salvador, J.J. Dannenberg, D.K. Malick, A.D. Rabuck, K. Raghavachari, J.B. Foresman, J. Cioslowski, J.V. Ortiz, A.G. Baboul, B.B. Stefanov, G. Liu, A. Liashenko, P. Piskorz, I. Komaromi, R. Gomperts, R.L. Martin, D.J. Fox, T. Keith, M.A. Al-Laham, C.Y. Peng, A. Nanayakkara, M. Challacombe, P.M.W. Gill, B. Johnson, W. Chen, M.W. Wong, J.L. Andres, C. Gonzalez, M. Head-Gordon, E.S. Replogle, and J.A. Pople, Gaussian, Inc., Pittsburgh PA, 2002.
[25] J.C. Ramílez, C.S. Rodolfo, O. Esquivel, P.R. Sagar, Phys. Rev. B 56 (1997) 4477.